



LAWRENCE
LIVERMORE
NATIONAL
LABORATORY

Applications in the Nuclear Industry for Thermal Spray Amorphous Metal and Ceramic Coatings

J. Blink, J. Choi, J. Farmer

July 9, 2007

Materials Science & Technology 2007 Conference and
Exhibition
Detroit, MI, United States
September 16, 2007 through September 20, 2007

Disclaimer

This document was prepared as an account of work sponsored by an agency of the United States Government. Neither the United States Government nor the University of California nor any of their employees, makes any warranty, express or implied, or assumes any legal liability or responsibility for the accuracy, completeness, or usefulness of any information, apparatus, product, or process disclosed, or represents that its use would not infringe privately owned rights. Reference herein to any specific commercial product, process, or service by trade name, trademark, manufacturer, or otherwise, does not necessarily constitute or imply its endorsement, recommendation, or favoring by the United States Government or the University of California. The views and opinions of authors expressed herein do not necessarily state or reflect those of the United States Government or the University of California, and shall not be used for advertising or product endorsement purposes.

Applications in the Nuclear Industry for Thermal Spray Amorphous Metal and Ceramic Coatings

J. Blink, J. Choi and J. Farmer

Lawrence Livermore National Laboratory, Livermore, California USA

Keywords: Iron-Based, Amorphous Metal, Coatings, Applications

Abstract

Amorphous metal and ceramic thermal spray coatings have been developed that can be used to enhance the corrosion resistance of containers for the transportation, aging and disposal of spent nuclear fuel and high-level radioactive wastes. Iron-based amorphous metal formulations with chromium, molybdenum and tungsten have shown the corrosion resistance believed to be necessary for such applications. Rare earth additions enable very low critical cooling rates to be achieved. The boron content of these materials, and their stability at high neutron doses, enable them to serve as high efficiency neutron absorbers for criticality control. Ceramic coatings may provide even greater corrosion resistance for container applications, though the boron-containing amorphous metals are still favored for criticality control applications. These amorphous metal and ceramic materials have been produced as gas atomized powders and applied as near full density, non-porous coatings with the high-velocity oxy-fuel process. This paper summarizes the performance of these coatings as corrosion-resistant barriers, and as neutron absorbers. Relevant corrosion models are also discussed, as well as a cost model to quantify the economic benefits possible with these new materials.

Introduction

The outstanding corrosion resistance that may be possible with amorphous metals was recognized several years ago [1-3]. Compositions of several iron-based amorphous metals were published, including several with very good corrosion resistance. Examples included: thermally sprayed coatings of Fe-10Cr-10-Mo-(C,B), bulk Fe-Cr-Mo-C-B, and Fe-Cr-Mo-C-B-P [4-6]. The corrosion resistance of an iron-based amorphous alloy with yttrium (Y), $\text{Fe}_{48}\text{Mo}_{14}\text{Cr}_{15}\text{Y}_2\text{C}_{15}\text{B}_6$ was also been established [7-9]. Yttrium was added to this alloy to lower the critical cooling rate. Several nickel-based amorphous metals were developed that exhibit exceptional corrosion performance in acids, but are not considered in this study, which focuses on iron-based amorphous metals. Thermal spray coatings of crystalline nickel-based alloy coatings have been deposited with thermal spray technology, but appear to have less corrosion resistance than comparable nickel-based amorphous metals [10].

A family of iron-based amorphous metals with very good corrosion resistance has been developed that can be applied as a protective thermal spray coating. One of the most promising formulations within this family was found to be $\text{Fe}_{49.7}\text{Cr}_{17.7}\text{Mn}_{1.9}\text{Mo}_{7.4}\text{W}_{1.6}\text{B}_{15.2}\text{C}_{3.8}\text{Si}_{2.4}$ (SAM2X5), which included chromium (Cr), molybdenum (Mo), and tungsten (W) for enhanced corrosion resistance, and boron (B) to enable glass formation and neutron absorption [11-15]. The parent alloy for this series of amorphous alloys, which is known as SAM40 and represented by the formula $\text{Fe}_{52.3}\text{Cr}_{19}\text{Mn}_2\text{Mo}_{2.5}\text{W}_{1.7}\text{B}_{16}\text{C}_4\text{Si}_{2.5}$, has less molybdenum than SAM2X5 and was

originally developed by Branagan [16-17]. In addition to SAM2X5, yttrium-containing SAM1651 ($\text{Fe}_{48}\text{Mo}_{14}\text{Cr}_{15}\text{Y}_2\text{C}_{15}\text{B}_6$) has also been explored

Possible Applications

SAM2X5 may have beneficial applications such as the safe long-term storage of spent nuclear fuel. These materials have exceptional neutron absorption characteristics, and are stable at high dose. The absorption cross section in transmission for thermal neutrons for SAM2X5 coatings is three to four times (3 to 4 \times) greater than that of borated stainless steel, and twice (2 \times) as good as nickel-based Alloy C-4 with additions of Gd (Ni-Cr-Mo-Gd) [18-20]. It may be possible to achieve substantial cost savings by substituting these new Fe-based materials for more expensive Ni-Cr-Mo and Ni-Cr-Mo-Gd alloys. Thermal spray coatings of Fe-based amorphous metals are predicted to cost \sim \$7 per pound, whereas plates of Ni-Cr-Mo are expected to cost \geq \$37 per pound, based upon actual purchase costs of Alloy C-22 (UNS # N06022), without additions of gadolinium.

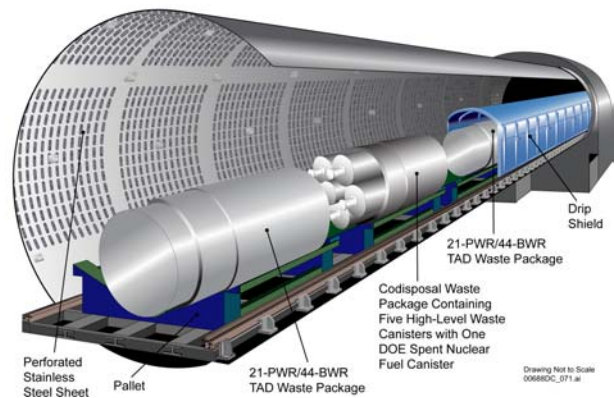


Figure 1. Three-dimensional illustration of containers for spent nuclear fuel and high-level radioactive wastes in typical drift (tunnel) at the Yucca Mountain site. Containers are protected from dripping water and falling rocks by the drip shield.

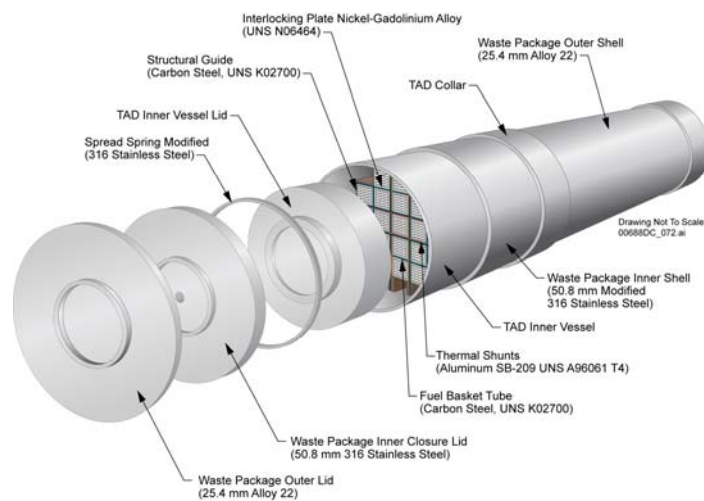


Figure 2. More detailed representation of spent nuclear fuel container, sized to accommodate 21-PWR fuel assemblies. The fuel basket tubes include neutron absorbers.

The hardness values for Type 316L stainless steel, nickel-based Alloy C-22, and HVOF SAM2X5 are 150, 250 and 1100-1300 VHN, respectively. These materials are extremely hard and provide enhanced resistance to abrasion and gouges. In fact, successful tests have been conducted for applications as disk cutters for the tunnel boring machines (Figure 3).



Figure 3. Face of tunnel boring machine exiting Yucca Mountain after construction of the initial tunnel, which is known as the Exploratory Studies Facility (ESF).

Thermal Spray Coatings

The coatings discussed here were made with the high-velocity oxy-fuel (HVOF) process (Figure 4), which involves a combustion flame, and is characterized by gas and particle velocities that are three to four times the speed of sound (mach 3 to 4). This process is ideal for depositing metal and cermet coatings, which have typical bond strengths of 5,000 to 10,000 pounds per square inch (5-10 ksi), porosities of less than one percent ($< 1\%$) and extreme hardness. The cooling rate that can be achieved in a typical thermal spray process such as HVOF are on the order of ten thousand Kelvin per second (10^4 K/s), and is high enough to enable many alloy compositions to be deposited above their respective critical cooling rate, thereby maintaining the vitreous state. However, the range of amorphous metal compositions that can be processed with HVOF is more restricted than those that can be produced with melt spinning, due to the differences in achievable cooling rates. Both kerosene and hydrogen have been investigated as fuels in the HVOF process used to deposit SAM2X5 and SAM1651. Type 316L stainless-steel cylinders were coated with SAM2X5, and served as half-scale models of containers for the storage of spent nuclear fuel. SAM2X5-coated cylinders and plates were subjected to eight (8) full cycles in the GM salt fog test. The results of salt-fog testing are discussed in a subsequent section of this paper. Cylinders have also been coated with the Y-containing SAM1651 and tested.

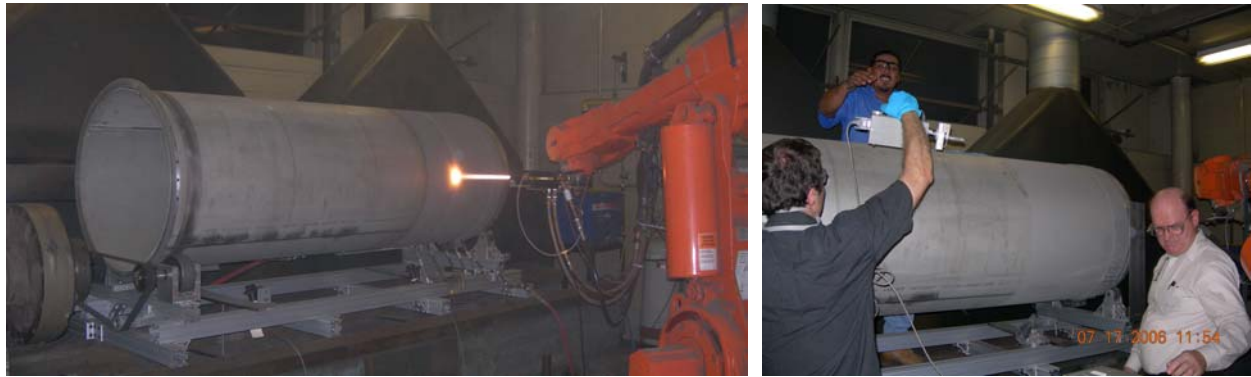


Figure 4. High-velocity oxy-fuel process at Caterpillar used to coat half-scale containers with SAM1651 amorphous metal. The torch is shown in the left frame, and quality assurance checks of the coating thickness and roughness are shown in the right frame.

Corrosion Performance

Samples Used for Immersion and Salt Fog Testing

A wide variety of standardized coating samples were made for corrosion testing, as shown in Figure 5. Samples of the powders used are in the bottles at the top. Crevice samples with a bolt hole in the center are shown on the left. Alloy C-22 rods coated with SAM2X5 and SAM1651 used to monitor open-circuit corrosion potentials and corrosion rates, as determined with linear polarization, are shown on the right. Weight loss samples used for long-term immersion testing are shown in the front center. Ultra-thick (~ 0.75 cm) coatings are also shown, slightly to the right of center.

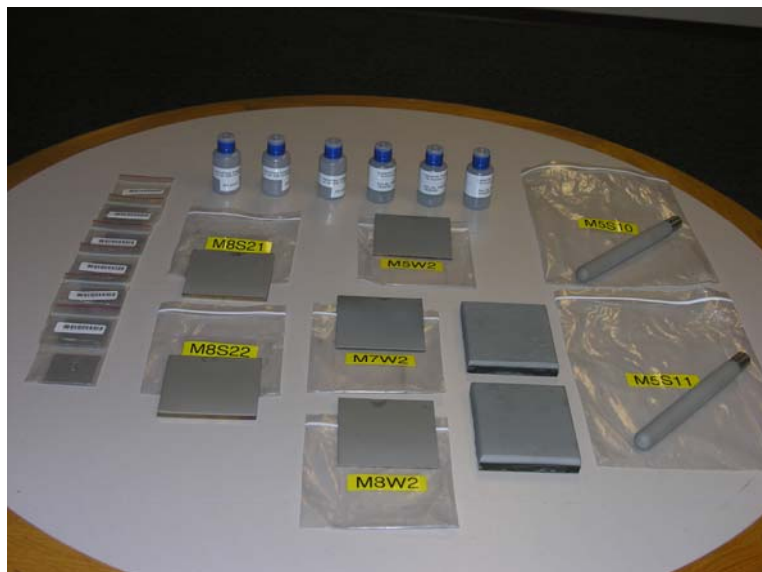


Figure 5. Samples of amorphous-metal HVOF coatings used for long-term corrosion testing.

Verification of Amorphous Nature of Powder and Coatings

X-ray diffraction (XRD) measurements of SAM2X5 powder (Lot # 06-015) and thermal-spray coatings made by depositing the powder on Type 316L stainless steel substrates (Figure 6). Similar results were also achieved with Alloy C-22 substrates. In regard to the thermal spray coating, the broad halo observed at $2\theta \sim 44^\circ$ indicated that the coating was predominately amorphous, and the small sharp peaks are attributed to the presence of minor crystalline phases [21-22]. These phases are believed to include Cr_2B , WC, M_{23}C_6 and bcc ferrite, which are known to have a detrimental effect on corrosion performance. These potentially deleterious precipitates deplete the amorphous matrix of those alloying elements, such as chromium, responsible for enhanced passivity. Coatings with less residual crystalline phase have been observed.

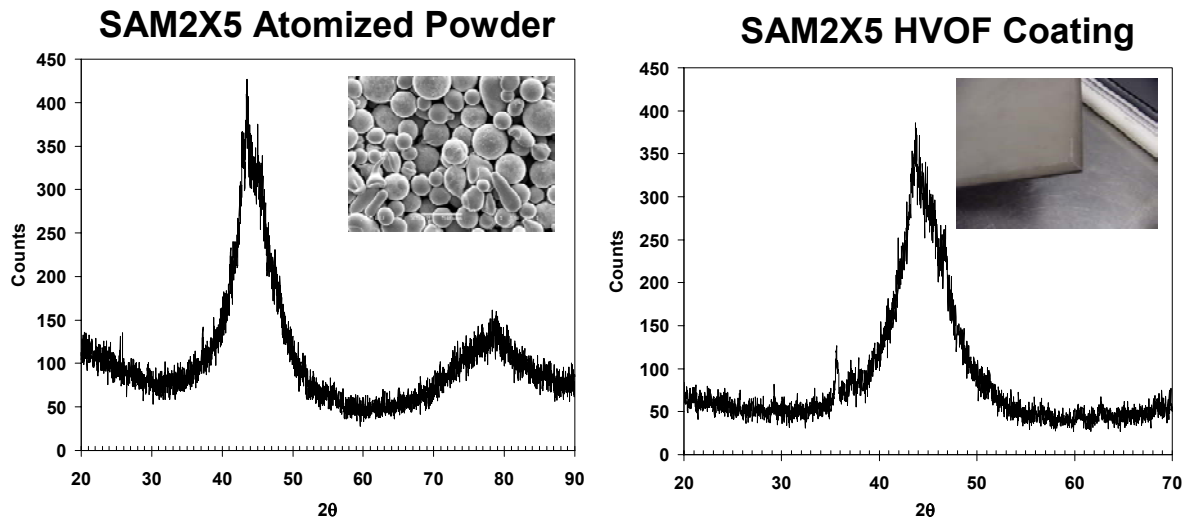


Figure 6. X-ray diffraction data for amorphous SAM2X5 powder (left) and coating produced from that powder (right) on a stainless steel substrate. Corrosion performance depends upon the amorphous nature of the material, and is compromised by the presence of Cr_2B , WC, M_{23}C_6 and bcc ferrite.

Solutions Used for Long-Term Immersion Tests

Ground water in the proposed repository at Yucca Mountain has been classified in three general categories, depending upon the terminal compositions that evolve during evaporative concentration: These categories include: calcium-chloride; sulfate-chloride; and bicarbonate. In general, the calcium-chloride brines are the most aggressive, and the bicarbonate brines are the least aggressive. Samples from the exploratory wells at Yucca Mountain fall into all of water-type categories, as shown in Figure 7. Standardized test solutions have therefore been developed which also fall into each ground water category. These synthetic brines were based upon concentrated J-13 well water, and are known as simulated dilute water (SDW), simulated concentrated water (SCW), and simulated acidic water (SAW) [23-27].

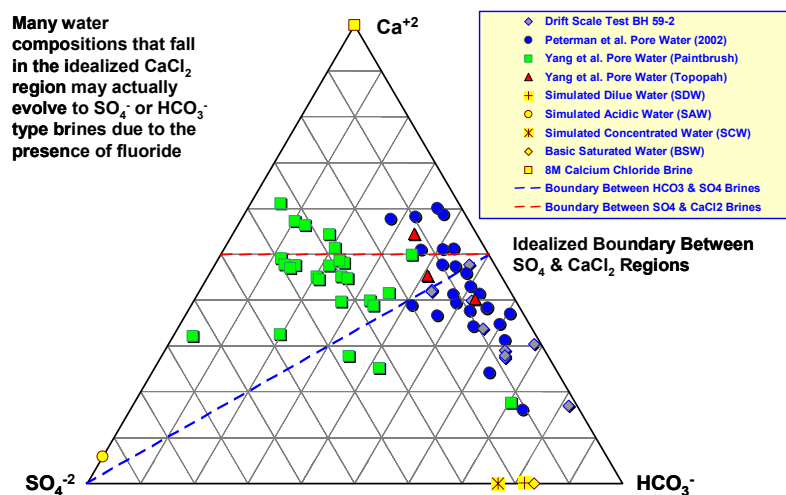


Figure 7. Ground water in the proposed underground repository at Yucca Mountain has been classified as calcium chloride brine; sulfate-chloride brine, or bicarbonate brine.

Results of Long-Term Immersion Tests

Initially, linear polarization was used to determine the corrosion rates of SAM2X5 coatings and wrought Alloy C-22 in several environments, including natural seawater and 5M CaCl₂ at 105°C, after an immersion of a few days. Table 1 shows that the rates determined for Alloy C-22 and SAM2X5 are comparable under these conditions.

Table 1. Corrosion Rates of Alloy C-22 and SAM2X5 HVOF Coatings in Seawater

Environment	Sample	E _{corr} (mV vs. SSC)	Corrosion Rate (µm/year)
30°C Seawater	HVOF SAM2X5	-87.4	0.18
30°C Seawater	Wrought Alloy C-22	-163.2	0.09
90°C Seawater	HVOF SAM2X5	-241.0	1.58
90°C Seawater	Wrought Alloy C-22	-318.2	1.22
105°C 5M CaCl ₂	HVOF SAM2X5	-240.9	2.70
105°C 5M CaCl ₂	Wrought Alloy C-22	-464.3	5.04
105C 5M CaCl ₂	HVOF Alloy C-22	-347.9	115.70

Long term weight-loss and dimensional-change data for SAM2X5 was also needed. After 135 days immersion, weight-loss and dimensional measurements were used to determine the corrosion rates of SAM2X5 coatings on Alloy C-22 weight-loss samples (Figure 8). Depending upon the assumed coating density, these rates were determined to be: (1) 14.3-15.9 µm/yr in natural seawater at 90°C; (2) 8.4-9.3 µm/yr in 3.5-molal NaCl solution at 30°C; (3) 26.1-29.7 µm/yr in 3.5-molal NaCl solution at 90°C; (4) 4.6-5.1 µm/yr in 3.5-molal NaCl and 0.525-molal KNO₃ solution at 90°C; (5) 8.3-9.4 µm/yr in SDW at 90°C; (6) 2.8-3.0 µm/yr in SCW at 90°C; and (7) 16.5-18.1 µm/yr in SAW at 90°C. As expected, greater corrosion rates were observed at higher temperature, and nitrate anion inhibited the corrosion of these iron-based materials in concentrated chloride solutions. Corrosion rates in bicarbonate-type brines were less than those in concentrated chloride solutions.

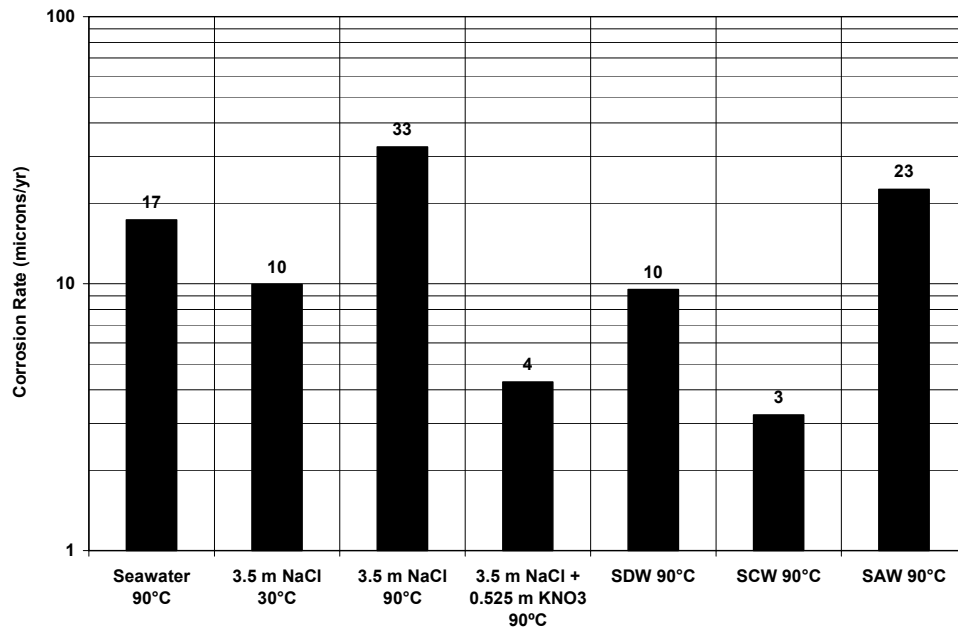


Figure 8. Corrosion rates of amorphous SAM2X5 coatings, based upon weight loss and dimensional changes measured after 135-day immersion test.

Salt Fog Performance

Salt fog tests were conducted according to the standard General Motors (GM) salt fog test, identified as GM9540P [11]. Thermal-spray coatings of SAM2X5 and SAM1651 coatings were tested, with 1018 steel samples serving as controls. After eight cycles in this salt-fog test, SAM2X5 and SAM1651 coatings on flat plates and a half-scale spent nuclear fuel (SNF) prototypical container proved to be corrosion resistant, whereas the steel reference samples underwent aggressive attack (Figures 9 and 10). In the case of the SAM1651-coated container, some running rust was observed on the bottom of the container, which may be due to surface preparation prior to coating (Figure 10).



Figure 9. Effect of GM9540P salt-fog test on 1018 steel reference samples (top), HVOF coating of SAM1651 amorphous metal on 316L and C-22 substrates (bottom right and left), and half-scale SNF prototypical container (bottom center).



Figure 10. Effect of GM9540P salt-fog test on HVOF coating of SAM1651 amorphous metal on half-scale SNF prototypical container (bottom center).

Neutron Absorption

The high boron content of $\text{Fe}_{49.7}\text{Cr}_{17.7}\text{Mn}_{1.9}\text{Mo}_{7.4}\text{W}_{1.6}\text{B}_{15.2}\text{C}_{3.8}\text{Si}_{2.4}$ (SAM2X5) make it an effective neutron absorber, and suitable for criticality control applications. Average measured values of the neutron absorption cross section in transmission (Σ_t) for Type 316L stainless steel, Alloy C-22, borated stainless steel, a Ni-Cr-Mo-Gd alloy, and SAM2X5 have been determined to be approximately 1.1, 1.3, 2.3, 3.8 and 7.1 cm^{-1} , respectively [19-20]. SAM2X5 and its parent alloy have been shown to maintain corrosion resistance up to the glass transition temperature, and to remain in the amorphous state after receiving relatively high neutron dose.

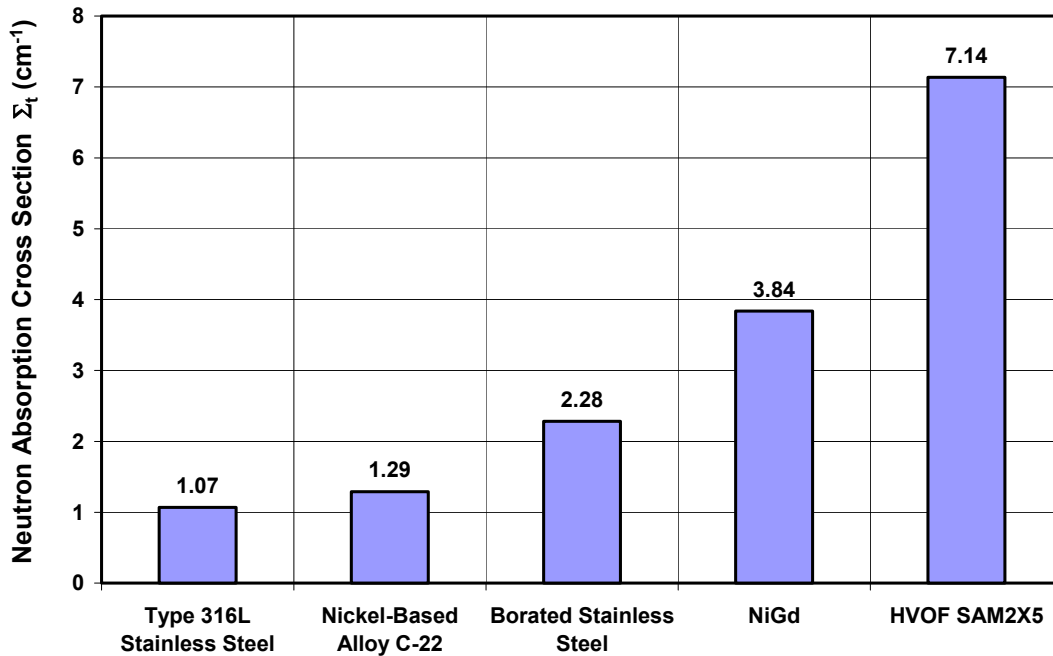


Figure 11. Average measured values of the neutron absorption cross section in transmission (Σ_t) for Type 316L stainless steel, Alloy C-22, borated stainless steel, a Ni-Cr-Mo-Gd alloy, and SAM2X5.

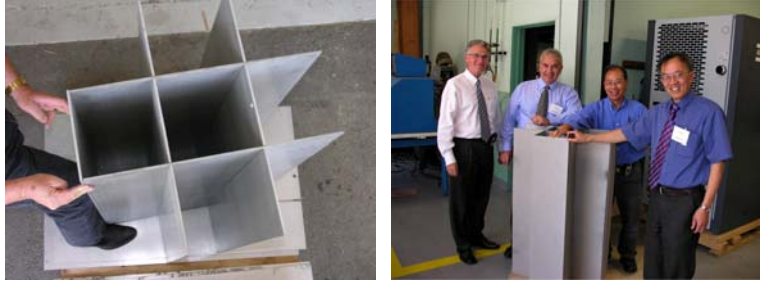


Figure 12. Prototypical half-scale half-length basket assembly, sized to fit inside the half-scale containers. After fabrication by water-jet cutting (left), and after coating with SAM2X5 (right).

Simulations and design calculations at LLNL show that k -effective can be lowered by at least ten percent (10 %) with the application of 1-millimeter thick coating of SAM2X5 to SNF support structure (basket) in a 21-PWR assembly waste container (Figures 1 and 12). Even better performance is possible through the use of enriched boron for the synthesis of the Fe-based amorphous metal. The Fe-based amorphous metals have already been produced in multi-ton quantities and should cost less than \$10 per pound, while relatively few (three-or-four) 300-pound heats have been made of the Ni-Gd Material, which may cost nearly \$40 per pound.

Economic Benefits

A cost model was developed and used to predict the cost to produce nickel-based alloys, including Type 316 stainless steel, as well as nickel-based Alloys C-276 and C-22. This cost model used raw materials data compiled by the United States Geological Survey (USGS), and represented graphically in Figure 13.

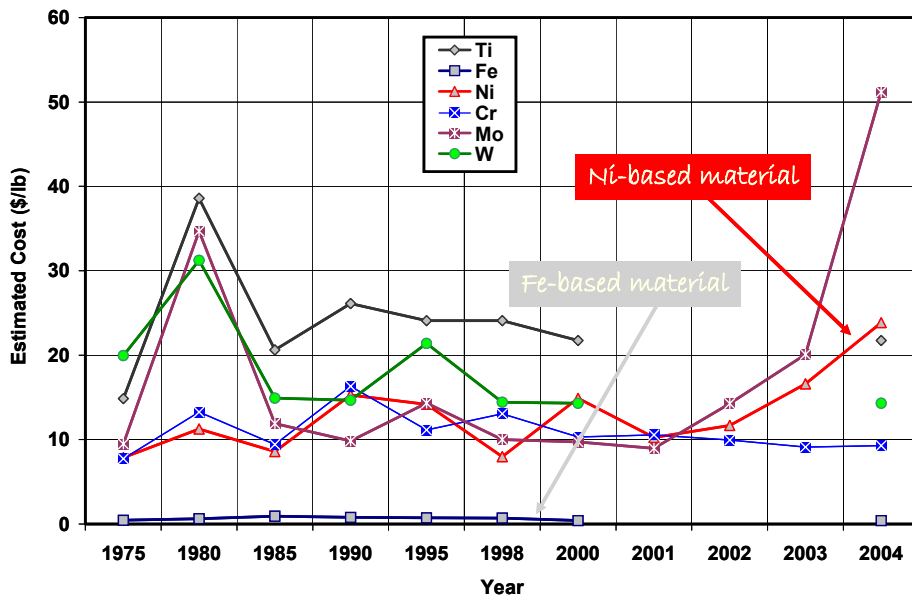


Figure 13. Cost of raw materials required for the production of Type 316L stainless steel, Alloy C-22, Fe-based amorphous metals, and titanium alloys. These costs were taken from the United States Geological Survey (USGS) web site, where raw materials are tracked [28].

This cost model also made the following assumptions:

1. Throughput = 1 waste package, 1 pallet, 1 drip shield per day
2. Floor Space = 75,000 square feet at \$500 per square foot
3. Personnel = 15 FTE at \$250,000 per person per year
4. Equipment = 39 HVOF guns (30 lb/hr) at \$250,000 per gun
5. Feed Cost = \$3/lb (Possible); \$ 6/lb (Mid Range); \$8/lb (Bounding)
6. Cost of Nickel-Based Wrought Alloy Increasing Rapidly

Based upon this model, the estimated raw-materials costs for nickel-based Alloys C-276 and C-22 were \$22-23/lb. The most recent procurements of Alloy C-22 plates by these authors was at a cost of \$37/lb. More exotic nickel-based alloys proposed for use as criticality control materials, such as Ni-Cr-Mo-Gd will cost even more due to the incorporation of gadolinium as a neutron poison. The cost of Type 316L stainless steel is estimated to be approximately \$7/lb. HVOF coatings of SAM2X5 and SAM1651 are predicted to cost \$10 and \$15 per pound, respectively (Figure 14).

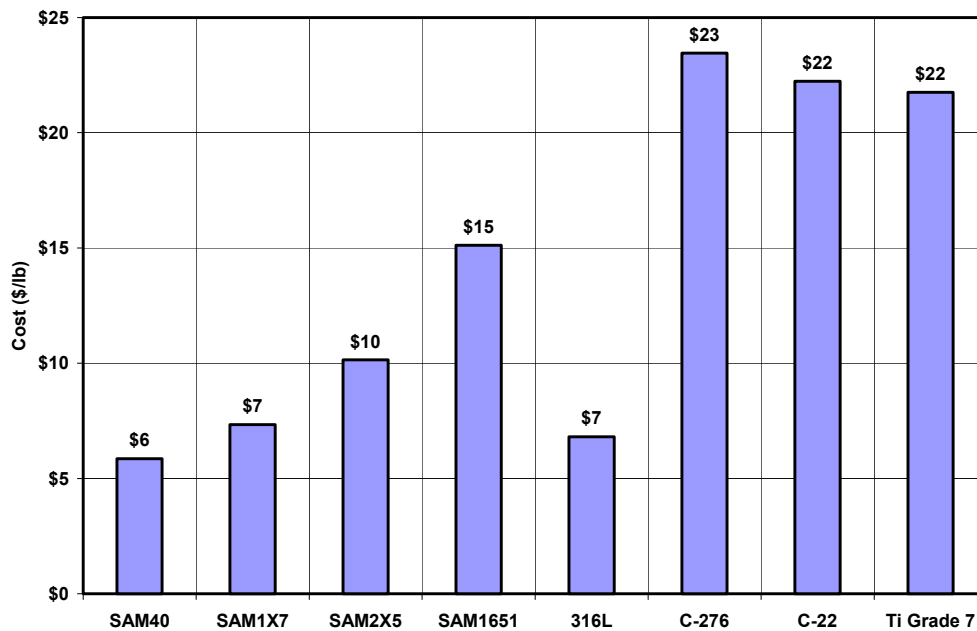


Figure 14. Estimates of finished materials costs, based upon the cost model, assumptions, and raw materials costs.

Assuming acceptable materials performance, the following cost savings could be achieved through substitution of an iron-based material for the more expensive nickel-based materials now specified for fabrication of SNF and HLW containers and pallets, and for titanium alloys now specified for fabrication of drip shields, all required for emplacement at the proposed repository at Yucca Mountain:

1. Assume \$3/lb: Substantial savings are realized for the ~11,000 waste packages (42%, \$881 million), pallets (24%, \$41 million), and drip shields (81%, \$2.8 billion).
2. Assume \$6/lb: Reasonable savings (7%, \$271 million) for the waste package, no savings for the pallet, and large savings for the drip shield (70%, \$2.5 billion).
3. Assume \$8/lb: No savings are achieved for the waste package or pallet, but substantial savings can still be realized for the drip shield (63%, \$2.3 billion).

Conclusions

Early Fe-based amorphous metal coatings had very poor corrosion resistance and failed salt-fog tests. The HPCRM Program has developed new Fe-based amorphous-metal alloys with good corrosion resistance, high hardness, and exceptional absorption cross-sections for thermal neutrons. More than forty high-performance Fe-based amorphous alloys were systematically designed and synthesized. Cr, Mo and W were added to enhance corrosion resistance; Y was added to lower the critical cooling rate; and B was added to render the alloy amorphous and to enhance capture thermal neutrons. Enriched boron could be used for the further enhancement of the absorption of thermal neutrons. Phase stability has been demonstrated well above 500-600°C and at high neutron dose (equivalent to 4000 years inside YM container). With additional development, these materials could be used to achieve cost benefits for the fabrication of next-generation spent nuclear fuel containers, and basket assemblies with enhanced criticality safety. Multi-ton quantities of gas-atomized SAM2X5 and SAM1651 powder have been produced and applied as protective coatings on numerous prototypes and parts. These new materials are now under evaluation for several applications of national importance. These applications include: (1) corrosion-resistant anti-skid decking for ships and (2) criticality control material for repository

Acknowledgments

This work was performed under the auspices of the U. S. DOE, UC, LLNL under Contract W-7405-Eng-48.

Work was co-sponsored by the Office of Civilian and Radioactive Waste Management (OCRWM) of the United States Department of Energy (DOE), and the Defense Science Office (DSO) of the Defense Advanced Research Projects Agency (DARPA). The guidance of Jeffrey Walker at DOE OCRWM and Leo Christodoulou at DARPA DSO is gratefully acknowledged. The production of gas atomized powders by The NanoSteel Company and Carpenter Powder Products, and the production of coatings from these powders by Plasma Technology Incorporated and Caterpillar are gratefully acknowledged.

References

- [1] M. Telford, The Case for Bulk Metallic Glass. *Materials Today*, Vol. 3, 2004, pp. 36-43
- [2] N. Sorensen and R. Diegle, Corrosion of Amorphous Metals, *Corrosion, Metals Handbook*, 9th Ed., Vol. 13, edited by J. R. Davis and J. D. Destefani, ASME, 1987, pp. 864-870
- [3] D. Polk and B. Giessen, Overview of Principles and Applications, Chapter 1, *Metallic Glasses*, edited by J. Gilman and H. Leamy, ASME, 1978, pp. 2-35
- [4] K. Kishitake, H. Era, and F. Otsubo, Characterization of Plasma Sprayed Fe-10Cr-10Mo-(C,B) Amorphous Coatings, *J. Thermal Spray Tech.*, Vol. 5 (No. 2), 1996, pp. 145-153
- [5] S. Pang, T. Zhang, K. Asami, and A. Inoue, Effects of Chromium on the Glass Formation and Corrosion Behavior of Bulk Glassy Fe-Cr-Mo-C-B Alloys, *Materials Transactions*, Vol. 43 (No. 8), 2002, pp. 2137-2142
- [6] S. Pang, T. Zhang, K. Asami, and A. Inoue, Synthesis of Fe-Cr-Mo-C-B-P Bulk Metallic Glasses with High Corrosion Resistance, *Acta Materialia*, Vol. 50, 2002, pp. 489-497
- [7] F. Guo, S. Poon, and G. Shiflet, Metallic Glass Ingots Based on Yttrium, *Metallic Applied Physics Letters*, Vol. 83 (No. 13), 2003, pp. 2575-2577
- [8] Z. Lu, C. Liu, and W. Porter, Role of Yttrium in Glass Formation of Fe-Based Bulk Metallic Glasses, *Metallic Applied Physics Letters*, Vol. 83 (No. 13), 2003, pp. 2581-2583
- [9] V. Ponnambalam, S. Poon, and G. Shiflet, *JMR*, Vol. 19 (No. 5), 2004, pp. 1320
- [10] D. Chidambaram, C. Clayton, and M. Dorfman, Evaluation of the Electrochemical Behavior of HVOF-Sprayed Alloy Coatings, *Surface and Coatings Technology*, Vol. 176, 2004, pp. 307-317
- [11] J. Farmer, J. Haslam, S. Day, T. Lian, C. Saw, P. Hailey, J. Choi, R. Rebak, N. Yang, J. Payer, J. Perepezko, K. Hildal, E. Lavernia, L. Ajdelsztajn, D. Branagan, Corrosion Resistance of Thermally Sprayed High-Boron Iron-Based Amorphous-Metal Coatings: Fe_{49.7}Cr_{17.7}Mn_{1.9}Mo_{7.4}W_{1.6}B_{15.2}C_{3.8}Si_{2.4}, UCRL-TR-227111 Rev. 1, LLNL, Livermore, CA; 2007; JMR-2007-0058, MRS, 2007, Accepted for Publication.
- [12] J. Farmer, J. Haslam, S. Day, T. Lian, C. Saw, P. Hailey, J. Choi, N. Yang, C. Blue, W. Peter, J. Payer and D. Branagan, Corrosion Resistances of Iron-Based Amorphous Metals with Yttrium and Tungsten Additions in Hot Calcium Chloride Brine and Natural Seawater, Fe₄₈Mo₁₄Cr₁₅Y₂C₁₅B₆ and W-containing Variants, Critical Factors in Localized Corrosion 5, A Symposium in Honor of Hugh Issacs, 210th ECS Meeting, edited by N. Missert, ECS Transactions, Vol. 3, ECS, 2006

- [13] J. Farmer, J. Haslam, S. Day, T. Lian, C. Saw, P. Hailey, J. Choi, R. Rebak, N. Yang, R. Bayles, L. Aprigliano, J. Payer, J. Perepezko, K. Hildal, E. Lavernia, L. Ajdelsztajn, D. J. Branagan, and M. B. Beardseley, A High-Performance Corrosion-Resistant Iron-Based Amorphous Metal – The Effects of Composition, Structure and Environment on Corrosion Resistance, Scientific Basis for Nuclear Waste Management XXX, Symposium NN, MRS Symposium Series, Vol. 985, 2006
- [14] J. Farmer, J. Haslam, S. Day, T. Lian, R. Rebak, N. Yang, L. Aprigliano, Corrosion Resistance of Iron-Based Amorphous Metal Coatings, PVP2006-ICPVT11-93835, ASME, New York, NY, 2006
- [15] J. Farmer, J. Haslam, S. Day, D. Branagan, C. Blue, J. Rivard, L. Aprigliano, N. Yang, J. Perepezko, M. Beardsley, Corrosion Characterization of Iron-Based High-Performance Amorphous-Metal Thermal-Spray Coatings, PVP2005-71664, ASME, New York, NY, 2005
- [16] D. Branagan, Method of Modifying Iron-Based Glasses to Increase Crystallization Temperature Without Changing Melting Temperature, U.S. Pat. Appl. No. 20040250929, Filed Dec. 16, 2004
- [17] D. Branagan, Properties of Amorphous/Partially Crystalline Coatings. U.S. Pat. Appl. No. 20040253381, Filed Dec. 16, 2004
- [18] T. Lian, D. Day, P. Hailey, J-S. Choi, and J. Farmer, Comparative Study on the Corrosion Resistance of Fe-Based Amorphous Metal, Borated Stainless Steel and Ni-Cr-Mo-Gd Alloy, Scientific Basis for Nuclear Waste Management XXX, Symposium NN, MRS Series, Vol. 985, 2006
- [19] J-S. Choi, C. Lee, J. Farmer, D. Day, M. Wall, C. Saw, M. Boussoufi, B. Liu, H. Egbert, D. Branagan, and A. D'Amato, Application of Neutron-Absorbing Structural Amorphous Metal Coatings for Spent Nuclear Fuel Container to Enhance Criticality Safety Controls, Scientific Basis for Nuclear Waste Management XXX, Symposium NN, MRS Symposium Series, Vol. 985, 2006
- [20] J. C. Farmer, J-S. Choi, C-K. Saw, R. H. Rebak, S. D. Day, T. Lian, P. D. Hailey, J. H. Payer, D. J. Branagan, L. F. Aprigliano, Corrosion Resistance of Amorphous $\text{Fe}_{49.7}\text{Cr}_{17.7}\text{Mn}_{1.9}\text{Mo}_{7.4}\text{W}_{1.6}\text{B}_{15.2}\text{C}_{3.8}\text{Si}_{2.4}$ Coating, A New Criticality Control Material, UCRL-JRNL-229505, LLNL, Livermore, CA; J. Nuclear Technology, ANS, 2007, Submitted for Publication
- [21] C. K. Saw, X-ray Scattering Techniques for Characterization Tools in the Life Sciences, Nanotechnologies for the Life Science, edited by Challa Kumar, Wiley-VCH Verlag GmbH and Company, KGaA, Weinheim, 2006
- [22] C. K. Saw and R. B. Schwarz, Chemical Short-Range Order in Dense Random-Packed Models, J. Less-Common Metals, Vol. 140, 1988, pp. 385-393

- [23] J. E. Harrar, J. F. Carley, W. F. Isherwood, and E. Raber, Report of the Committee to Review the Use of J-13 Well Water in Nevada Nuclear Waste Storage Investigations, UCID-21867, LLNL, Livermore, CA, 1990
- [24] G. E. Gdowski, Formulation and Make-up of Simulated Dilute Water (SDW), Low Ionic Content Aqueous Solution, YMP TIP-CM-06, Rev. CN TIP-CM-06-0-2, LLNL, Livermore, CA, 1997
- [25] G. E. Gdowski, Formulation and Make-up of Simulated Concentrated Water (SCW), High Ionic Content Aqueous Solution, YMP TIP-CM-07, Rev. CN TIP-CM-07-0-2, LLNL, Livermore, CA, 1997
- [26] G. E. Gdowski, Formulation and Make-up of Simulated Acidic Concentrated Water (SAW), High Ionic Content Aqueous Solution, YMP TIP-CM-08, Rev. CN TIP-CM-08-0-2, LLNL, Livermore, CA, 1997
- [27] J. Farmer, S. Lu, D. McCright, G. Gdowski, F. Wang, T. Summers, P. Bedrossian, J. Horn, T. Lian, J. Estill, A. Lingenfelter, W. Halsey, General and Localized Corrosion of High-Level Waste Container in Yucca Mountain, Transportation, Storage, and Disposal of Radioactive Materials, ASME, PVP Vol. 408, 2000, pp. 53-70
- [28] Mineral Commodity Summaries, United States Geological Survey (USGS), January, 2005: *Iron and Steel* – M. Fenton; *Cobalt* – K. B. Shedd; *Nickel* – P. H. Kuck; *Chromium* – J. F. Papp; *Molybdenum* – M. J. Magyar and J. W. Blossom; *Tungsten* – K. B. Shedd; *Manganese* – T. S. Jones; *Titanium* – J. Gambogi.